Approximate treatment of relativistic effects in the low-energy $\alpha + \alpha$ scattering

L. C. Chamon,[1] L. R. Gasques,[1] and B. V. Carlson[2]
[1]*Departamento de Física Nuclear, Instituto de Física da Universidade de São Paulo, Caixa Postal 66318, 05315-970 São Paulo, SP, Brazil.*
[2]*Departamento de Física, Instituto Tecnológico de Aeronáutica, Centro Técnico Aeroespacial, São José dos Campos, SP, Brazil*
(Received 16 August 2011; published 13 October 2011)

We develop a method to describe approximately the effects of relativity in low-energy scattering of identical nuclei. The method results in an equation similar to the Schrödinger one, but with modified (effective) energy and potential. The model is applied to the elastic scattering data analyses of the $\alpha + \alpha$ system. We demonstrate that the effects of relativity are not totally negligible in this case even at very low energies. We also develop a new parametrization of the effective nucleon-nucleon interaction that can be extended to other systems.

DOI: 10.1103/PhysRevC.84.044607 PACS number(s): 24.10.Ht, 25.55.Ci, 24.10.Jv

I. INTRODUCTION

Quantum mechanics and relativity are the pillars of modern physics. Even so, the effects of relativity have been neglected when analyzing data obtained from the collision of nuclei at low energies. This procedure seems appropriate because of the corresponding low (asymptotic) velocities in comparison with the speed of light. However, due to the strong attractive nuclear potential, at small separation distances the local relative velocity of the nuclei can reach significant values and, then, relativity could provide significant effects. This fact is not important in the case of heavy-ion systems because the internal distances are not probed in elastic scattering data analyses due to the corresponding strong absorption. On the other hand, the $\alpha + \alpha$ system has no significant reaction channels at low energies and, therefore, the elastic scattering for this system is sensitive to the interaction even at very small distances. In the present paper, we demonstrate that the data analyses for this system are rather sensitive to the effects of relativity even at very low energies.

Heavy-ion elastic scattering data have been analyzed in the context of the usual Schrödinger equation for many systems over a wide energy range. The phenomenological potential strengths obtained in these analyses present a strong energy dependence. Several models have been developed to account for this dependence. In particular, the São Paulo potential (SPP) [1] is a theoretical model for the nuclear interaction in which this energy dependence is associated with Pauli nonlocality. The SPP has been successfully applied in data analyses of several reaction channels, for many heavy-ion systems and in a very wide energy range. As the $\alpha + \alpha$ system has different characteristics in relation to the heavy-ion reactions, in an earlier work [2] we tested the SPP in the elastic scattering data analyses for $\alpha + \alpha$. In that work, we discussed extensively several properties of heavy-ion, α-nucleus, and α-α systems. Therefore, in the present paper we provide only a brief review of the main features of the $\alpha + \alpha$ system.

At low bombarding energies, the reaction channels for the $\alpha + \alpha$ system present negligible cross sections. In fact, for bombarding energies below 34.6 MeV, the only open reaction channel corresponds to the ^{4}He(^{4}He,γ)^{8}Be process with a very small cross section [3–6]. Therefore, due to the lack of reaction channels, low-energy elastic scattering data analyses for $\alpha + \alpha$ must be realized without an imaginary part in the optical potential. Under this condition, the data analyses are sensitive to and, thus, probe the real part of the interaction at quite small distances. In the past, all the potentials proposed to describe the experimental phase shifts presented a strong ℓ dependence [7,8]. In 1977, Buck, Friedrich and Wheatley obtained a potential [9] that is independent of both energy and angular momentum and, by adjusting two parameters of the Gaussian shape assumed for the potential, they obtained a good description of the experimental phase shifts and also of the position and width of the s-wave resonance related to the unbound ^{8}Be ground state. In our recent analyses of $\alpha + \alpha$ elastic scattering with the SPP [2], we obtained a weak ℓ dependence of the normalization of the potential, which was necessary to fit the data. In that work, we proposed, without demonstration, that such a dependence could arise from effects of relativity not included in the corresponding theoretical calculations. This was the motivation of the present work.

A full relativistic approach to low-energy scattering should start from a relativistically covariant theory from which the nonrelativistic expressions and their relativistic corrections can be derived. We consider, however, that the main effects of relativity at low energies are related to the variation of mass and length contraction (of the nuclear densities) as functions of the velocity of the nuclei. Thus, in the next section we develop a model to account for these two effects of relativity. Then, in Sec. III, we apply this model to elastic scattering data analyses of the $\alpha + \alpha$ system at low energies. Nevertheless, even considering the effects of relativity, the present work shows that the SPP still needs an ℓ-dependent normalization to reproduce the data. Thus, in Sec. IV we propose a new parametrization of the effective nucleon-nucleon interaction to account for the $\alpha + \alpha$ elastic scattering data in the context of the relativistic approach.

II. THE MODEL

When considering the nonrelativistic scattering of two identical particles of mass m_0, with reduced mass $\mu_0 = m_0/2$, the laboratory (LAB) and center of mass (CM) energies are

related by

$$E_{\rm CM} = E_{\rm LAB}/2. \quad (1)$$

In the case of a potential with spherical symmetry, $V_S(R)$, the nonrelativistic Schrödinger equation can be written as

$$[\hat{K} + V_S(R)]\Psi = E_{\rm CM}\Psi, \quad (2)$$

where the kinetic energy operator is given by

$$\hat{K} = \frac{\hat{p}^2}{2\mu_0} \rightarrow -\frac{\hbar^2}{2\mu_0}\frac{\partial^2}{\partial R^2} + \frac{\ell(\ell+1)\hbar^2}{2\mu_0 R^2}. \quad (3)$$

This results in the usual expansion in partial waves:

$$-\frac{\hbar^2}{2\mu_0}\frac{\partial^2\Psi_\ell}{\partial R^2} + \frac{\ell(\ell+1)\hbar^2}{2\mu_0 R^2}\Psi_\ell + V_S(R)\Psi_\ell = E_{\rm CM}\Psi_\ell. \quad (4)$$

The total potential is a sum of the Coulomb and nuclear interactions: $V_S(R) = V_{\rm SC}(R) + V_{\rm SN}(R)$. This potential can be obtained through a folding procedure involving the nuclear densities:

$$V(R) = \int \rho_1(\vec{r}_1)\rho_2(\vec{r}_2)v(\vec{R} - \vec{r}_1 + \vec{r}_2)\,d\vec{r}_1\,d\vec{r}_2. \quad (5)$$

In the case of the Coulomb interaction, Eq. (5) involves the charge distributions of the nuclei and the fundamental electromagnetic interaction between two pointlike charges: $v(\vec{R}) = e^2/R$. The SPP [1] can be assumed for the nuclear interaction. In this case, Eq. (5) involves the matter distributions of the nuclei and

$$v(\vec{R}) = N_R\, V_0\delta(\vec{R})e^{-4v_{\rm REL}^2/c^2}, \quad (6)$$

with $V_0 = -456$ MeV fm^3, where c is the speed of light and $v_{\rm REL}$ represents the local relative velocity between the two nuclei. The matter distribution of the nucleus represents a folding of the corresponding nucleon density with the intrinsic matter distribution of the nucleon and, therefore, it takes into account the size of the nucleon [1]. We emphasize that the velocity dependence of Eq. (6) is related to the effects of Pauli nonlocality [1,10,11] and thus it does not arise from the effects of relativity. N_R in Eq. (6) is a normalization factor that we use to fit the data. We call the standard SPP the case in which $N_R = 1$. In this work, the charge density assumed for the α nucleus was obtained from electron scattering experiments, according to Ref. [12]. The α matter distribution is obtained by multiplying the charge density by a factor of 2. That is, we have assumed the neutron matter density to be equal to the proton charge density. To test this hypothesis, we performed self-consistent relativistic mean-field calculations for the α nucleus using the NL3 [14] and DDME1 [15] parametrizations of the interaction. In both cases, we found the rms radius of the neutron distribution to be only 0.7% smaller than that of the proton distribution, which we believe justifies our use of equal neutron and proton matter densities.

The Klein-Gordon equation represents a possible approach to the problem of relativistic scattering of spinless particles. On the other hand, if the potential is much smaller than the rest mass, which is the present case, it is known that the Klein-Gordon equation can be approximated by the Schrödinger one. This result is expected owing to the correspondence principle: a new theory must agree with the old theory in the old one's regime of validity. Thus, in the present work we include in the Schrödinger equation two main effects of relativity: the variation of mass with velocity and length contraction. The main purpose of this procedure is that it allows a quite simple and practical interpretation of the effects of relativity.

The relativistic relation between the LAB and CM energies is derived in Appendix A and is represented by Eq. (A4). Due to relativistic length contraction, the nuclear densities are deformed, which affects the potential, as extensively discussed latter. For now, we denote the potential from the deformed densities by $V_D(R)$. Taking into account Eq. (A6), in the relativistic case we assume an equation similar to Eq. (2), but with $V_D(R)$ replacing $V_S(R)$. Since we are not dealing with extremely large velocities, we treat the effects of relativity as a perturbation of the Schrödinger equation. Thus, based on Eqs. (A11) and (A12), we propose the following:

$$-\frac{\hbar^2}{2\mu}\frac{\partial^2\Psi_\ell}{\partial R^2} + \frac{\ell(\ell+1)\hbar^2}{2\mu R^2}\Psi_\ell + V_D(R)\Psi_\ell = E_{\rm CM}\Psi_\ell, \quad (7)$$

where

$$\mu = \frac{\mu_0}{\left(1 - \frac{1}{16}\frac{v_{\rm REL}^2}{c^2} - \frac{1}{128}\frac{v_{\rm REL}^4}{c^4}\right)}. \quad (8)$$

The local relative velocity between the nuclei is related to the potential by [see (A8)]

$$\frac{v_{\rm REL}^2}{c^2} = 4\left[1 - \left(\frac{4\mu_0 c^2}{4\mu_0 c^2 + E_{\rm CM} - V_D(R)}\right)^2\right]. \quad (9)$$

In the present case of low energies, the variation of the mass represented by Eq. (8) is very small. In fact, even at small separation distances, where the potential reaches large (negative) strengths, μ differs from μ_0 by less than 1%.

Asymptotically ($R \rightarrow \infty$), the potential vanishes and the asymptotic relative velocity is given by

$$\left(\frac{v_{\rm REL}^2}{c^2}\right)_{As} = 4\left[1 - \left(\frac{4\mu_0 c^2}{4\mu_0 c^2 + E_{\rm CM}}\right)^2\right]. \quad (10)$$

Thus, we define the effective energy as

$$E_{\rm EFF} = E_{\rm CM}\left[1 - \frac{1}{16}\left(\frac{v_{\rm REL}^2}{c^2}\right)_{As} - \frac{1}{128}\left(\frac{v_{\rm REL}^4}{c^4}\right)_{As}\right]. \quad (11)$$

With this, Eq. (7) can be rewritten as

$$-\frac{\hbar^2}{2\mu_0}\frac{\partial^2\Psi_\ell}{\partial R^2} + \frac{\ell(\ell+1)\hbar^2}{2\mu_0 R^2}\Psi_\ell + V_{\rm EFF}(R)\Psi_\ell = E_{\rm EFF}\Psi_\ell, \quad (12)$$

where the two first terms now involve the reduced rest mass, and the effective potential is given by

$$V_{\rm EFF}(R) = V_D(R)\left(1 - \frac{1}{16}\frac{v_{\rm REL}^2}{c^2} - \frac{1}{128}\frac{v_{\rm REL}^4}{c^4}\right) + E_{\rm CM}\left\{\frac{1}{16}\left[\frac{v_{\rm REL}^2}{c^2} - \left(\frac{v_{\rm REL}^2}{c^2}\right)_{As}\right] + \frac{1}{128}\left[\frac{v_{\rm REL}^4}{c^4} - \left(\frac{v_{\rm REL}^4}{c^4}\right)_{As}\right]\right\}. \quad (13)$$

As demonstrated in Appendix B, the effective potential is proportional to $1/R$ for large R values. The method of calculating the deformed potential is described in Appendices B and C. The ℓ dependence of the effective potential is demonstrated in Appendix C.

Before proceeding with the data analyses, we discuss the effects of relativity on the present case of the $\alpha + \alpha$ system at low energies. The correction of the energy represented by Eq (11) is very small (less than 0.1%), so essentially we have $E_{\rm EFF} = E_{\rm CM}$. The main effect of relativity is thus related to the difference between the effective potential and the spherical one: $\Delta V(R) = V_{\rm EFF}(R) - V_S(R)$. In the present region of low energies, the term involving $E_{\rm CM}$ in Eq. (13) is negligible and $\frac{1}{128}\frac{v_{\rm REL}^4}{c^4} \ll \frac{1}{16}\frac{v_{\rm REL}^2}{c^2}$, as well. Thus, we obtain $\Delta V \approx V_D(1 - \frac{1}{16}\frac{v_{\rm REL}^2}{c^2}) - V_S(R)$. Two effects are present in this equation: the deformation of the potential due to length contraction and the variation of mass with velocity. Figure 1(a) shows the spherical potential in the case of the $\alpha + \alpha$ system at $E_{\rm LAB} = 20$ MeV. Figure 1(b) presents the corresponding local relative velocity. In Figs. 1(c) and 1(d) we show, for $\ell = 0$ and $\ell = 4$, $100 \times \Delta V(R)/V_S(R)$ of the nuclear and Coulomb interactions, respectively. The effective nuclear potential differs from the spherical one by about 1%. This result indicates that some small effect of relativity could be observed in the elastic scattering process for this system, since it is very sensitive to the interaction.

In our model we have included the effects of relativity up to the order $v_{\rm REL}^4/c^4$. The main purpose of this procedure was to verify that the contribution of terms in $v_{\rm REL}^4/c^4$ is much smaller than that of terms in $v_{\rm REL}^2/c^2$. This condition, necessary to make the expansion in terms of velocity valid, was satisfied in our calculations (except, of course, in regions where the contribution of $v_{\rm REL}^2/c^2$ vanishes).

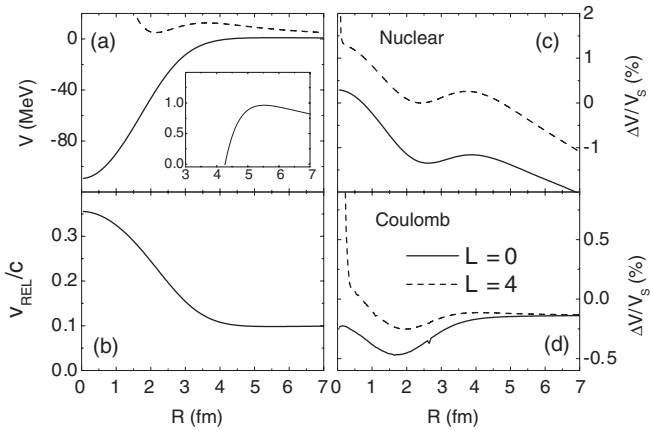

FIG. 1. (a) Spherical potential (nuclear + Coulomb) for the $\alpha + \alpha$ system at $E_{\rm LAB} = 20$ MeV. The solid and dashed lines correspond to $\ell = 0$ and $\ell = 4$, respectively. In the case of $\ell = 4$, the centrifugal contribution was summed with the spherical potential. The inset shows the region of the s-wave barrier. (b) Relative velocity between the nuclei (in units of c) as a function of the distance. (c) and (d) $100 \times \Delta V(R)/V_S(R)$ for the nuclear and Coulomb interactions, respectively. The calculations were performed for $\ell = 0$ (solid lines) and $\ell = 4$ (dashed lines).

III. DATA ANALYSES

Hereafter, we call the classical approach that involving the solution of the usual (nonrelativistic) Schrödinger equation with the spherical potential. We refer to the solution of Eq. (12) with the ℓ-dependent effective potential as the relativistic approach. As already discussed, due to the lack of reaction channels for the $\alpha + \alpha$ system, we do not use an imaginary part in the optical potential. The SPP is adopted for the nuclear interaction, with a normalization [N_R of Eq. (6)] assumed to fit the data. Of course, as we consider the SPP a realistic model, we should obtain $N_R \approx 1$.

As commented earlier in Ref. [2], we analyzed a large set of low-energy $\alpha + \alpha$ elastic scattering data within the classical approach. Nevertheless, instead of Eq. (9), in that work we assumed a different expression to obtain the relative velocity (Eq. (3) of [2]), which is involved in the calculations of the SPP. The results obtained in the classical approach with Eq. (9) are in fact very similar to those obtained in Ref. [2] but with slightly different N_R values. In order to be consistent in the comparison between relativistic and classical results, in the present work we provide the classical results obtained using Eq. (9).

^{8}Be is the compound nucleus in an $\alpha + \alpha$ collision. The ^{8}Be ground state is unbound, with an experimental Q value (relative to the 2α channel) of about 92 keV and a width of about 6 eV. These properties can be taken into account in the theoretical calculations, by fitting the corresponding s-wave resonance. In order to reproduce these values within the classical approach, it is necessary to assume a normalization factor of $N_R = 1.09692$ while within the relativistic approach we obtained $N_R = 1.10201$. Therefore, even at this extremely low energy ($E_{\rm CM} \approx 0.1$ MeV), the effects of relativity are significant enough to provide a difference of about 0.5% between the N_R values of the classical and relativistic approaches.

Figure 2 shows experimental phase shifts obtained from elastic scattering data analyses in Refs. [13,16–19]. In this low-energy region, the data fits are sensitive only to the $\ell = 0, 2$, and 4 phase shifts. In order to describe these data within the context of the classical approach, it is necessary to assume different N_R values for different ℓ waves, as illustrated in Fig. 2(a). We emphasize that such an ℓ dependence is weak, since the N_R values vary by only about 3.3% from $\ell = 0$ to $\ell = 4$. This weak ℓ dependence inspired the present work, since we believed that it could arise from the effects of relativity. Nevertheless, as presented in Fig. 2(b), in order to fit the experimental phase shifts in the relativistic approach, the N_R values correspond to a slightly reduced but a still nonnegligible weak ℓ dependence (about 2.5% from $\ell = 0$ to $\ell = 4$).

The $\alpha + \alpha$ elastic scattering at low energies represents an exceptional probe of the nuclear interaction. Indeed, due to the complete lack of absorption, the data are very sensitive to the real part of the optical potential. Furthermore, no complications arising from couplings or the spin-orbit interaction are present in this case. Therefore, this system represents a more fundamental theoretical context in relation to heavy-ion systems, for which the imaginary part of the optical potential causes ambiguities in the determination (from data

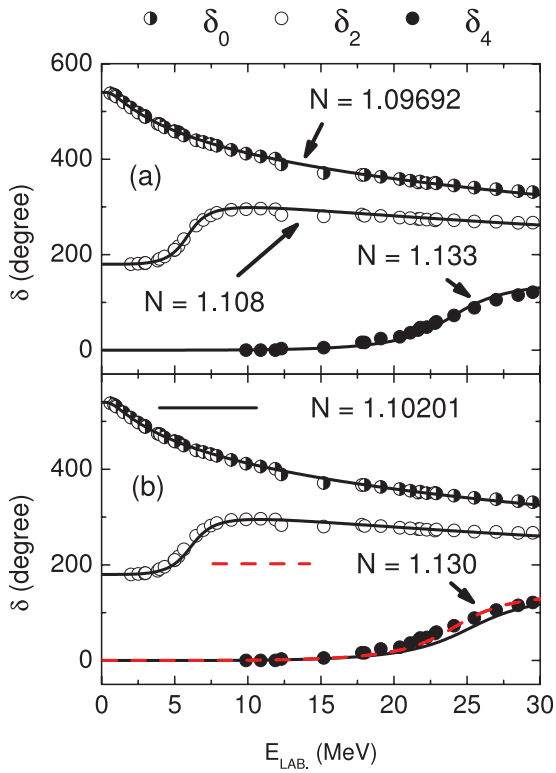

FIG. 2. (Color online) Comparison between experimental phase shifts (from Refs. [13,16–19]), for $L = 0$, 2, and 4, with theoretical results of the classical (a) and relativistic (b) approaches. The normalization factors of the SPP assumed in the calculations are indicated in the figure.

analyses) of parameters of the real part. Thus, a quite accurate determination of the nuclear interaction for the $\alpha + \alpha$ system is very important. The importance of this subject would be increased even more if this interaction were independent of the energy and angular momentum but dependent on the nuclear densities, since then it could be easily extrapolated to other systems. As already commented, an energy- and ℓ-independent potential that accounts for the $\alpha + \alpha$ data was already obtained many years ago by Buck *et al.* [9]. However, in that case the interaction was not described in terms of the α densities. As demonstrated in Ref. [2], it is also possible to describe the data within the context of the SPP without any ℓ dependence in N_R, but in this case the shape of the α matter density must be different from that of the charge one. This fact is not totally satisfactory since the α charge density has been obtained quite accurately from electron scattering experiments. As already commented, both matter and charge densities already take into account the finite size of the nucleon [1]. Thus, since the number of neutrons is identical to the number of protons, the assumption that the matter density is twice that of the charge one should be precise for the α nucleus. Furthermore, both descriptions above (from Buck *et al.* [9] and SPP [9]) were performed within the classical approach. As we have demonstrated, relativistic effects are small but not totally negligible for the $\alpha + \alpha$ system. Thus, it is quite interesting to look for an interaction that describes the data in the context of the relativistic approach, without any further ℓ and energy dependencies besides those arising from relativity. Taking into account the considerations above, in the next section we describe a method that we have used to obtain a new model of the effective nuclear interaction.

IV. SEARCH FOR AN EFFECTIVE NUCLEAR INTERACTION

We have searched for the effective nuclear interaction $v(\vec{R} - \vec{r}_1 + \vec{r}_2)$ that is involved in the folding interaction of Eq. (5). In these calculations, we assumed, again, that the α matter density is twice the charge density. To determine $v(\vec{R})$, we performed a simultaneous fit of the experimental $L = 0$, 2, and 4 phase shifts and also of the position (92 keV) and width (6 eV) of the s-wave ^{8}Be resonance. The first attempt was performed with a zero-range approximation without the velocity dependence that arises from Pauli nonlocality: $v(\vec{R}) = V_0\,\delta(\vec{R})$, where V_0 was considered an ℓ-independent free parameter. We did not obtain good fits to the data with this model.

We then considered different trial functions with finite-range shapes:

$$v(\vec{r}) = -U_0\, f(r), \tag{14}$$

where the function $f(r)$ involves one parameter (a). For a determined trial function, we have varied (on a grid) the values of the corresponding a parameter. For each of these values, the U_0 parameter was adjusted in order to reproduce the ^{8}Be resonance. Then, considering the agreement between the theoretical and experimental phase shifts ($L = 0$, 2, and 4), we have determined the best parameter values.

The results obtained are summarized in Table I. All these functions provide very good and similar fits of the experimental phase shifts within the relativistic approach, as illustrated with solid lines in Fig. 3(b) for the first function (of Table I). A comparison among these functions is shown in Fig. 4(a). Clearly, they present quite different shapes. On the other hand, all of the functions provide very similar volume integrals ($V_0 = 418$ MeV fm^3 within 0.7% precision—see Table I) and also rather similar root-mean-square radii ($r_{\rm RMS} = 1.207$ fm within 6.5% precision). For the purpose of illustration, we also show, in Fig. 4(b), the corresponding effective nucleon-nucleon interactions obtained from Eq. (5). In these calculations, the matter distributions of the nucleon were considered identical to the charge density of the proton obtained from electron scattering experiments: an exponential shape with a diffuseness value of 0.235 fm [1].

TABLE I. Parameter (U_0 and a) values, volume integrals (V_0), and root-mean square radii ($r_{\rm RMS}$) of the trial functions $f(r)$.

	$f(r)$	U_0 (MeV)	a (fm)	V_0 (MeV fm^3)	$r_{\rm RMS}$ (fm)
1	$e^{-(r/a)^2}$	87.226	0.95	416.4	1.164
2	$e^{-r/a}$	330.61	0.37	420.9	1.282
3	$r\,e^{-(r/a)^2}$	161.22	0.80	414.9	1.131
4	$r\,e^{-r/a}$	1042.0	0.27	417.5	1.207

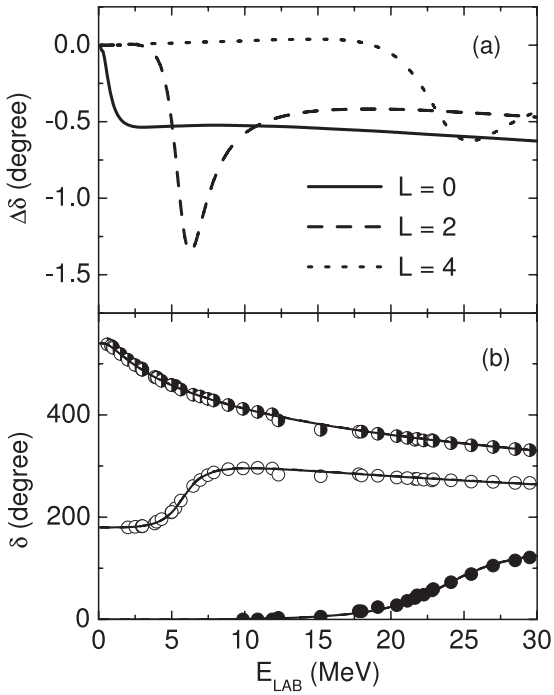

FIG. 3. (a) Difference between phase shifts calculated within the relativistic and classical approaches: $\Delta\delta = \delta_{\rm REL} - \delta_{\rm CLAS}$. (b) Comparison between experimental phase shifts (from Refs. [13,16–19]), for $L = 0, 2,$ and 4, with theoretical results of the relativistic approach. In the theoretical calculations, the first function of Table I has been assumed for the nuclear interaction.

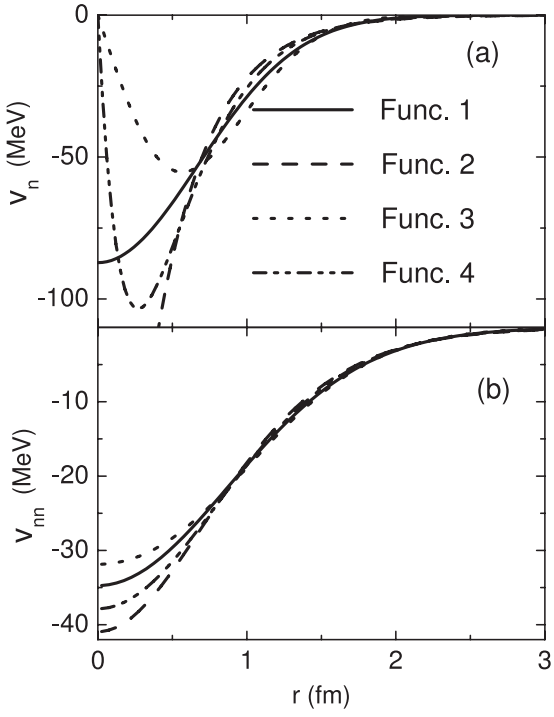

FIG. 4. (a) Comparison among the functions of Table I that provide good data fits of the experimental phase shifts in the context of the relativistic approach. (b) The corresponding effective nucleon-nucleon interactions obtained from Eq. (5) and considering an exponential shape for the matter density of the nucleon.

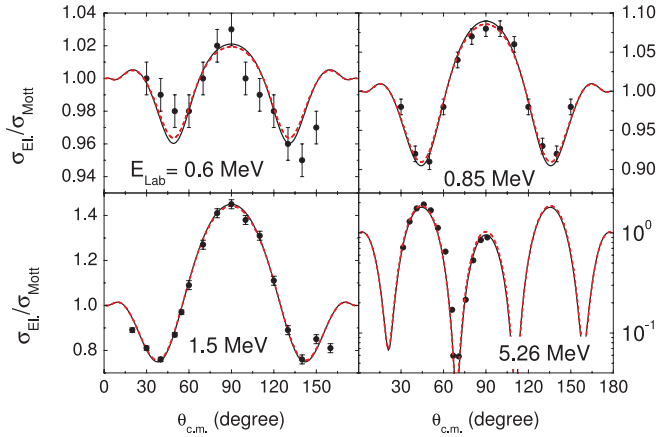

FIG. 5. (Color online) Experimental elastic scattering angular distributions compared to theoretical cross sections obtained with the nuclear interaction represented by function 1 of Table I. The solid and dashed lines were obtained within the relativistic and classical approaches, respectively.

In order to illustrate the effects of relativity, in Fig. 3(a) we show the difference between the phase shifts calculated within the relativistic and classical approaches, $\Delta\delta = \delta_{\rm REL} - \delta_{\rm CLAS}$, for $\ell = 0$, 2, and 4. Theoretical calculations of the elastic scattering cross sections are presented for several angular distributions in Figs. 5 and 6. Very small differences between the cross sections from the relativistic (solid lines) and the classical (dashed lines) approaches can be observed in these figures, mainly at the lower energies, due to the corresponding linear scales.

The characteristics of no absorption in the $\alpha + \alpha$ system, and consequently the lack of an imaginary potential in the interaction, is valid only at very low energies. Thus, we have not used our model to analyze higher energy data. However, just for curiosity, it is interesting to see what the effects of relativity predicted by our model would be at intermediate energies. Figure 7 shows the sum of the effective potential with the centrifugal one at $E = 50$, 100, and 200 MeV/nucleon for $\ell = 0$ and 4. For the purpose of comparison, the corresponding results for the spherical (classical) potential are also shown

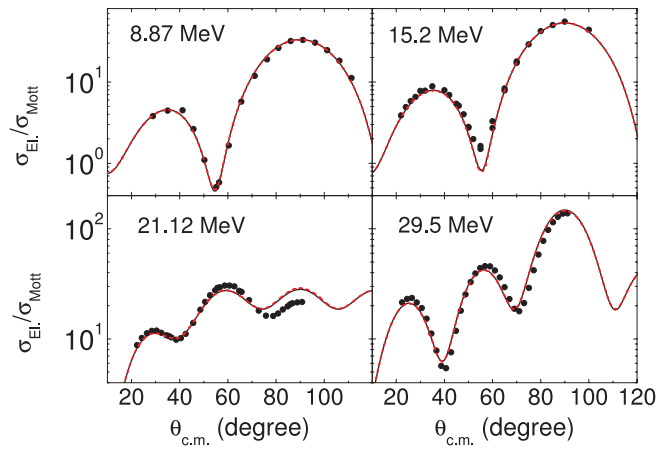

FIG. 6. (Color online) The same of Fig. 5 but for other energies.

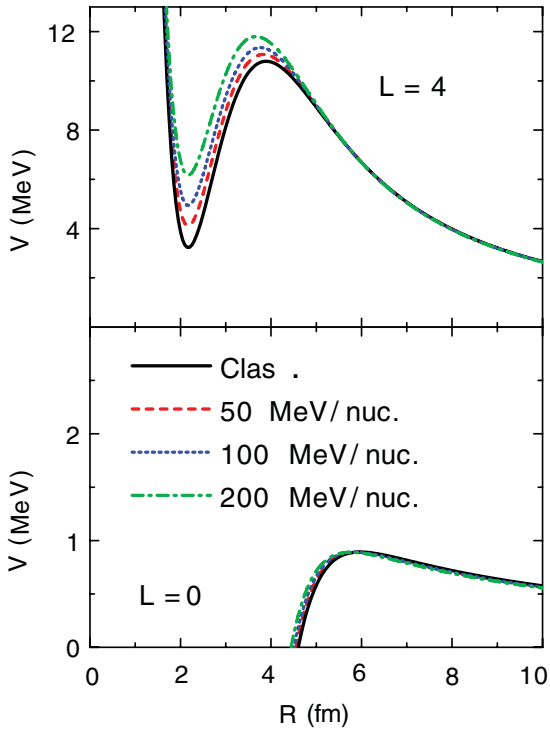

FIG. 7. (Color online) The sum of the effective and centrifugal potentials at different energies for $\ell = 0$ and 4. The corresponding results for the spherical potential are also shown.

in the figure. In these calculations, the first function of Table I was assumed for the nuclear interaction and, therefore, the energy dependence of the potentials comes only from relativistic effects. The barrier height for $\ell = 4$ becomes significantly larger for higher energies (see Fig. 7). On the other hand, the s-wave barrier height is almost not affected by relativity. The reason for this behavior is that, due to the short range, the contraction of space affects the nuclear potential more than the Coulomb one. The barrier radii for large ℓ values are smaller than those for small ℓ. At smaller distances, the nuclear potential is more intense and then relativity plays a more significant role. Based on the results presented in Fig. 7, we consider that our model indicates that the data analyses at these higher energies should be quite sensitive to the effects of relativity.

V. CONCLUSION

We have developed a method to take into account two relativistic effects in $\alpha + \alpha$ scattering: the variation of mass and length contraction related to the velocities of the nuclei. The main advantage of this procedure is that it results in a Schrödinger equation with an effective potential, which allows a clear and simple study of the effects of relativity. A full approach starting from a relativistically covariant theory could result in additional effects, but we believe that the main effects of relativity at low energies are those that we have considered in the present model. In the energy region studied here, the effective potential differs by about 1% from the nonrelativistic one at small distances of interaction. This effect mostly arises from relativistic length contraction, which affects the densities of the nuclei. This very small effect is observed in $\alpha + \alpha$ scattering only because the data are very sensitive to the real part of the optical potential. For example, in order to describe the properties of the ^{8}Be ground state, the normalization factor obtained for the nuclear potential in the relativistic approach varies by about 0.5% in relation to the value resulting from the classical approach. Within a general point of view, a variation of 0.5% is considered very small for most of the phenomena of nuclear physics. On the other hand, since we are dealing with relativistic effects at extremely low energies, $E_{\rm CM} \approx 0.1$ MeV (^{8}Be ground state), for which the asymptotic velocity is much smaller than the speed of light, $v^2_{\rm REL}/c^2 \approx 2E_{\rm CM}/\mu_0 c^2 \approx 10^{-4}$, even a variation of only 0.5% can sound remarkably large.

Characteristics of $\alpha + \alpha$ scattering at low energies, such as the complete lack of open reaction channels and the absence of a spin-orbit interaction, make the corresponding very precise elastic data set an exceptional probe of the nuclear interaction. Since the α density was accurately determined from electron scattering experiments, it is very interesting to obtain the nuclear interaction for the $\alpha + \alpha$ system expressed as a folding involving the nuclear density distributions. With this, the model could easily be extrapolated to other systems. Taking these points into account, we have also searched for an effective nuclear interaction that provides a good description of the experimental phase shifts within the relativistic approach. No other energy or ℓ dependence was assumed in the interaction besides that arising from relativity. As a result of this search, we obtained a set of functions with quite different shapes but with similar volume integrals and root-mean square radii.

As already commented, the present method of studying the effects of relativity uses approximations that should be valid as long as the velocities are not too high. Thus, we believe that our method can be extended to intermediate energies. For instance, at $E = 100$ Mev/nucleon the asymptotic velocity corresponds to $v^2_{\rm REL}/c^2 \approx 0.20$ and, therefore, contributions of higher order terms of the velocity to the interaction should be small. However, since in this energy region it is necessary to consider an imaginary part in the potential, we have not analyzed higher energy data. Even so, the results for the effective potential obtained from our simulations indicate that the effects of relativity should be significant at intermediate energies.

ACKNOWLEDGMENTS

This work was partially supported by the Fundação de Amparo à Pesquisa do Estado de São Paulo (FAPESP) and the Conselho Nacional de Desenvolvimento Científico e Tecnológico (CNPq).

APPENDIX A: SOME TOPICS IN RELATIVITY

In this Appendix, we consider the scattering of two identical particles with rest mass m_0 and provide several results that have been used in our work. The total energy in the laboratory

(LAB) frame is related to the laboratory energy ($E_{\rm LAB}$) through

$$E_{\rm TOT} = 2m_0c^2 + E_{\rm LAB}, \tag{A1}$$

where $E_{\rm LAB}$ is the asymptotic kinetic energy of the projectile and, therefore, is related to its asymptotic velocity:

$$E_{\rm LAB} = \frac{m_0c^2}{\sqrt{1 - v_{\rm LAB}^2/c^2}} - m_0c^2. \tag{A2}$$

The center-of-mass (CM) frame of reference has velocity $v_{\rm CM}$ relative to the LAB one and, of course, the asymptotic velocities of both particles in the CM frame are also equal to $v_{\rm CM}$. By considering the relativistic transformation of velocities, it is possible to obtain the relation

$$v_{\rm LAB} = \frac{2v_{\rm CM}}{1 + v_{\rm CM}^2/c^2}. \tag{A3}$$

The center-of-mass energy ($E_{\rm CM}$) can also be related to the asymptotic velocities of the two particles in the CM frame:

$$E_{\rm CM} = 2\left(\frac{m_0c^2}{\sqrt{1 - v_{\rm CM}^2/c^2}} - m_0c^2\right). \tag{A4}$$

Equations (A2), (A3), and (A4) result in the following relation between the CM and LAB energies:

$$E_{\rm CM} = 2m_0c^2[\sqrt{1 + E_{\rm LAB}/2m_0c^2} - 1]. \tag{A5}$$

Now we just consider the CM frame of reference. We define the reduced rest mass of the system by $\mu_0 = m_0/2$. The total energy is given by

$$E_{\rm TOT} = 2m_0c^2 + E_{\rm CM} = 2m_0c^2 + K(R) + V(R), \tag{A6}$$

where K is the kinetic energy and V represents the sum of the nuclear and Coulomb potentials. The kinetic energy is related to the local velocity of the particles (v) or to their local relative velocity ($v_{\rm REL} = 2v$) by

$$K = 2\left[\frac{m_0c^2}{\sqrt{1 - v^2/c^2}} - m_0c^2\right] = \frac{4\mu_0c^2}{\sqrt{1 - v_{\rm REL}^2/4c^2}} - 4\mu_0c^2. \tag{A7}$$

Equations (A7) and (A6) can be combined to give

$$\frac{v_{\rm REL}^2}{c^2} = 4\left[1 - \left(\frac{4\mu_0c^2}{4\mu_0c^2 + E_{\rm CM} - V(R)}\right)^2\right]. \tag{A8}$$

The momentum of each particle is given by

$$p = mv = \frac{m_0v}{\sqrt{1 - v^2/c^2}} = \frac{\mu_0v_{\rm REL}}{\sqrt{1 - v_{\rm REL}^2/4c^2}}. \tag{A9}$$

Thus, Eq. (A7) can be written as

$$K = \frac{p^2}{2\mu_0}\left[2 - \frac{8c^2}{v_{\rm REL}^2}\left(1 - \sqrt{1 - v_{\rm REL}^2/4c^2}\right)\right]. \tag{A10}$$

We expand this equation, retaining terms only to $v_{\rm REL}^4/c^4$, and obtain

$$K = \frac{p^2}{2\mu}, \tag{A11}$$

where we define

$$\mu = \frac{\mu_0}{\left(1 - \frac{1}{16}\frac{v_{\rm REL}^2}{c^2} - \frac{1}{128}\frac{v_{\rm REL}^4}{c^4}\right)}. \tag{A12}$$

Equations (A11) and (A12) reproduce the results of (A10) [and (A7)] quite accurately, within 0.016% for $0 \leqslant v_{\rm REL} \leqslant 0.7\,c$.

APPENDIX B: CALCULATION OF THE EFFECTIVE POTENTIAL

At low bombarding energies, the term involving $E_{\rm CM}$ in Eq. (13) is much smaller than that with $V_D(R)$. Thus, we can simplify this term (involving $E_{\rm CM}$) as follows, without loosing accuracy in the calculation of the effective potential. In general, the sum of the nuclear and Coulomb interactions is much smaller than the reduced rest mass. In fact, it is known that the depth of the nuclear potential is about 50 MeV/nucleon while m_0c^2 is about 1000 MeV/nucleon. Then, the strength of $V_D(R)$ in Eq. (9) is at most about 1/40 times $4\mu_0c^2$. Therefore, Eq. (9) can be expanded to provide

$$\frac{v_{\rm REL}^2}{c^2} \approx 4\left[1 - \left(\frac{4\mu_0c^2}{4\mu_0c^2 + E_{\rm CM}}\right)^2\right] - \frac{2V_D(R)/\mu_0c^2}{(1 + E_{\rm CM}/4\mu_0c^2)^3}$$

or

$$\frac{v_{\rm REL}^2}{c^2} - \left(\frac{v_{\rm REL}^2}{c^2}\right)_{As} \approx -\frac{2V_D(R)/\mu_0c^2}{(1 + E_{\rm CM}/4\mu_0c^2)^3}. \tag{B1}$$

Analogously, we obtain

$$\frac{v_{\rm REL}^4}{c^4} - \left(\frac{v_{\rm REL}^4}{c^4}\right)_{As} \approx -\frac{8[V_D(R)E_{\rm CM}/(\mu_0c^2)^2](1 + E_{\rm CM}/8\mu_0c^2)}{(1 + E_{\rm CM}/4\mu_0c^2)^5}. \tag{B2}$$

With this, Eq. (13) can be rewritten as

$$V_{\rm EFF}(R) \approx V_D(R)\left[1 - \frac{1}{16}\frac{v_{\rm REL}^2}{c^2} - \frac{1}{128}\frac{v_{\rm REL}^4}{c^4} - \frac{\epsilon(1 + 4\epsilon + 2\epsilon^2)}{2(1 + \epsilon)^5}\right], \tag{B3}$$

where $\epsilon = E_{\rm CM}/4\mu_0c^2$.

We now study the asymptotic behavior of the effective potential. For large R values, the nuclear potential vanishes and the Coulomb contribution is approximately the potential of two pointlike charges: $V_D(R) \approx Z^2e^2/R$. Furthermore, in this case (large R values), the velocities of Eq. (B3) can be approximated by their asymptotic values, and we obtain

$$V_{\rm EFF}(R) \approx \frac{Z^2e^2}{R}\left[1 - \frac{1}{16}\left(\frac{v_{\rm REL}^2}{c^2}\right)_{As} - \frac{1}{128}\left(\frac{v_{\rm REL}^4}{c^4}\right)_{As} - \frac{\epsilon\left(1 + 4\epsilon + 2\epsilon^2\right)}{2\left(1 + \epsilon\right)^5}\right], \tag{B4}$$

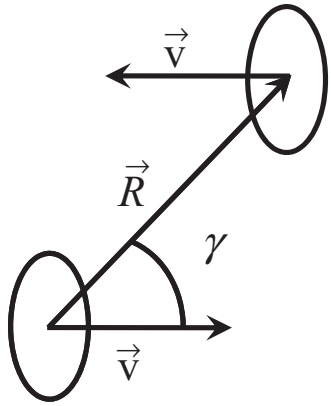

FIG. 8. Illustration of the collision of two identical nuclei in the CM frame of reference. The deformations of the densities arise from length contraction in the direction of the respective velocities.

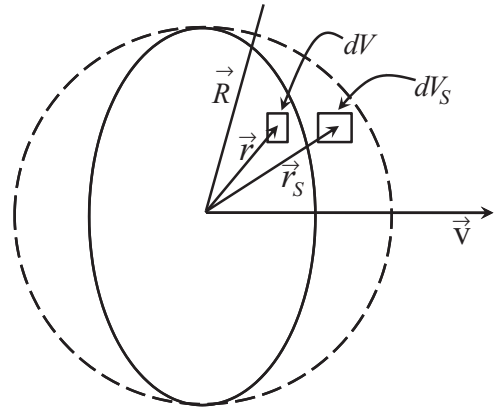

FIG. 9. Length contraction effect on density. The solid line represents the deformed density of a nucleus due to length contraction in the direction of its velocity. The dashed line represents the corresponding density without the effect of the contraction. The elements of volume with and without contraction are also represented in the figure.

or equivalently, in terms of the ϵ parameter,

$$V_{\rm EFF}(R) \approx \frac{Z^2e^2}{R}\left[1-\epsilon \times \frac{1+17\epsilon/4+17\epsilon^2/4+15\epsilon^3/8+3\epsilon^4/8}{(1+\epsilon)^5}\right]. \tag{B5}$$

Thus, for large R values the effective potential is proportional to $1/R$, which is the usual result for the Coulomb interaction (with a small renormalization of the charge).

We turn now to the calculation of $V_D(R)$. Figure 8 illustrates the collision of the two nuclei in the CM frame of reference. $\vec{R}$ connects the CM of the nuclei. The corresponding densities are compressed, due to length contraction in the direction of the respective velocities $\vec{v}$. The angle between $\vec{R}$ and $\vec{v}$, γ, is also represented in the figure. The solid line in Fig. 9 represents the deformed density of one of these nuclei. The dashed line in this figure represents the corresponding spherical density, i.e., without the effect of length contraction. The volume elements with (dV) and without (dV_S) considering the contraction are also represented in the figure in their corresponding positions $\vec{r}$ and $\vec{r}_S$. The Coulomb and nuclear interactions could be calculated through expression (5) by considering the deformed densities (hereafter, labeled by ρ). However, it is quite convenient to express these interactions in terms of the spherical densities ρ_S. In that follows, we show how we can reach this goal.

Due to charge conservation, the amount of charge of the spherical density within dV_S is equal to the amount of charge of the deformed density in dV. Thus $\rho(\vec{r})dV = \rho_S(r_S)dV_S$. On the other hand, due to length contraction, the volume elements are related by $dV_S = dV/\sqrt{1-v^2/c^2}$, where v is the velocity of the nucleus in the CM frame. Thus, we obtain the following relation:

$$\rho(\vec{r}) = \frac{\rho_S(r_S)}{\sqrt{1-v^2/c^2}}. \tag{B6}$$

As usual when calculating folding potentials, we assume the z axis to be in the direction of $\vec{R}$. By considering the contraction of the density in the direction of $\vec{v}$, as illustrated in Figs. 8 and 9, it is possible to demonstrate the following relation between the positions of the volume elements:

$$r_S = r\sqrt{1+\frac{v^2/c^2}{(1-v^2/c^2)}\left[\cos\gamma\cos\theta-\sin\gamma\sin\theta\cos\phi\right]^2}, \tag{B7}$$

where θ and ϕ are the angular coordinates of $\vec{r}$, and γ is the angle between $\vec{R}$ and $\vec{v}$ (see Fig. 8). In Appendix C we describe the method used to obtain the γ angle for each R value. With this, we obtain

$$V_D(R) = \frac{1}{(1-v^2/c^2)}\int \rho_S(r_{S1})\rho_S(r_{S2})v \times (\vec{R}-\vec{r}_1+\vec{r}_2)\,d\vec{r}_1\,d\vec{r}_2, \tag{B8}$$

where in the calculation of $\rho_S(r_S)$ it is necessary to take into account relation (B7).

Equation (B8) is a six-dimensional integral that takes much computer time in numerical calculations. Furthermore, it involves the velocities of the nuclei that depend on the potential through Eq. (9). The potential could be obtained by iteration but, in this case, Eq. (B7) must be calculated several times. To avoid this problem, we expand $\rho_S(r_S)$ [through Eq. (B7)] in powers of v/c up to fourth order:

$$\rho_S(r_S) \approx \rho_S(r) + rX\left\{\frac{v^2}{2c^2}\frac{\partial\rho_S(r)}{\partial r} + \frac{v^4}{8c^4}\left[rX\frac{\partial^2\rho_S(r)}{\partial r^2}+(4-X)\frac{\partial\rho_S(r)}{\partial r}\right]\right\}, \tag{B9}$$

where $X = [\cos\gamma\cos\theta-\sin\gamma\sin\theta\cos\phi]^2$.

By introducing Eq. (B9) in (B8) and taking into account that $v = v_{\rm REL}/2$, we obtain

$$V_D(R) = \frac{1}{\left(1 - v_{\rm REL}^2/4c^2\right)}\left[V_S(R) - \frac{v_{\rm REL}^2}{c^2}\Delta V_2(R) + \frac{v_{\rm REL}^4}{c^4}\Delta V_4(R)\right], \tag{B10}$$

where $V_S(R)$ is the spherical potential and

$$\Delta V_2(R) = -\frac{1}{4}\int r_1 X_1 \rho_S(r_2)\frac{\partial \rho_S(r_1)}{\partial r_1} v(\vec{R} - \vec{r}_1 + \vec{r}_2)\, d\vec{r}_1\, d\vec{r}_2, \tag{B11}$$

$$\Delta V_4(R) = \frac{1}{64}\int r_1 X_1 \left\{ r_2 X_2 \frac{\partial \rho_S(r_1)}{\partial r_1}\frac{\partial \rho_S(r_2)}{\partial r_2} + \rho_S(r_2)\left[r_1 X_1 \frac{\partial^2 \rho_S(r_1)}{\partial r_1^2} + (X_1 - 4)\frac{\partial \rho_S(r_1)}{\partial r_1}\right]\right\} \times v(\vec{R} - \vec{r}_1 + \vec{r}_2)\, d\vec{r}_1\, d\vec{r}_2, \tag{B12}$$

$$X_1 = \left[\cos\gamma\cos\theta_1 - \sin\gamma\sin\theta_1\cos\phi_1\right]^2, \tag{B13}$$

$$X_2 = \left[\cos\gamma\cos\theta_2 - \sin\gamma\sin\theta_2\cos\phi_2\right]^2. \tag{B14}$$

Finally, expanding Eqs. (B13) and (B14) and considering that a few of the corresponding terms in Eqs. (B11) and (B12) vanish due to symmetries, we obtain

$$\Delta V_2(R) = I_{20} + I_{22}\sin^2\gamma, \tag{B15}$$

$$\Delta V_4(R) = I_{40} + I_{42}\sin^2\gamma + I_{44}\sin^4\gamma, \tag{B16}$$

with the integrals

$$I_{20} = -\frac{1}{4}\int r_1 \cos^2\theta_1\, \rho_S(r_2)\frac{\partial \rho_S(r_1)}{\partial r_1} v(\vec{R} - \vec{r}_1 + \vec{r}_2)\, d\vec{r}_1\, d\vec{r}_2, \tag{B17}$$

$$I_{22} = -\frac{1}{4}\int r_1(\sin^2\theta_1\cos^2\phi_1 - \cos^2\theta_1)\rho_S(r_2)\frac{\partial \rho_S(r_1)}{\partial r_1} \times v(\vec{R} - \vec{r}_1 + \vec{r}_2)\, d\vec{r}_1\, d\vec{r}_2, \tag{B18}$$

$$I_{40} = \frac{1}{64}\int r_1\cos^2\theta_1\left\{ r_2\cos^2\theta_2\frac{\partial \rho_S(r_1)}{\partial r_1}\frac{\partial \rho_S(r_2)}{\partial r_2} + \rho_S(r_2)\left[r_1\cos^2\theta_1\frac{\partial^2\rho_S(r_1)}{\partial r_1^2} + (\cos^2\theta_1 - 4)\frac{\partial \rho_S(r_1)}{\partial r_1}\right]\right\} \times v(\vec{R} - \vec{r}_1 + \vec{r}_2)\, d\vec{r}_1\, d\vec{r}_2, \tag{B19}$$

$$I_{42} = \frac{1}{64}\int r_1\left\{ r_2[2\cos^2\theta_2(\cos^2\phi_1\sin^2\theta_1 - \cos^2\theta_1) + \cos\phi_1\cos\phi_2\sin(2\theta_1)\sin(2\theta_2)]\frac{\partial \rho_S(r_1)}{\partial r_1}\frac{\partial \rho_S(r_2)}{\partial r_2} + 2\rho_S(r_2)\left[(3\sin^2\theta_1\cos^2\phi_1 - \cos^2\theta_1)r_1\cos^2\theta_1\frac{\partial^2\rho_S(r_1)}{\partial r_1^2} + [\sin^2\theta_1\cos^2\phi_1(3\cos^2\theta_1 - 2) - \cos^2\theta_1(\cos^2\theta_1 - 2)] \times \frac{\partial \rho_S(r_1)}{\partial r_1}\right]\right\} v(\vec{R} - \vec{r}_1 + \vec{r}_2)\, d\vec{r}_1\, d\vec{r}_2, \tag{B20}$$

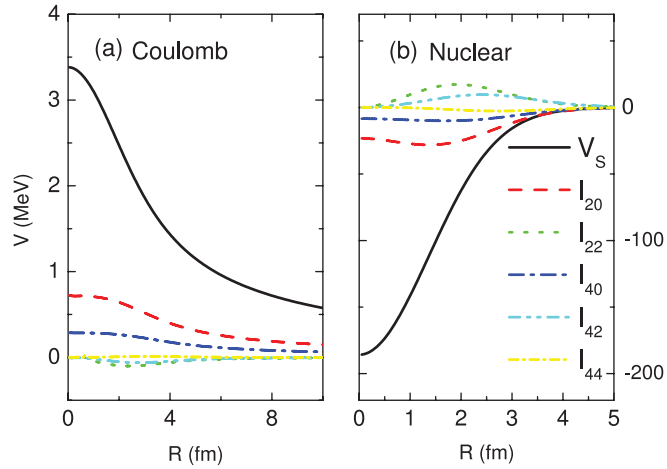

FIG. 10. (Color online) Components of the deformed potential for the (a) Coulomb and (b) nuclear contributions. The calculations for the nuclear part were performed without considering the velocity dependence of the SPP which arises from the Pauli nonlocality.

$$I_{44} = \frac{1}{64}\int r_1\left\{ r_2[\cos^2\theta_1\cos^2\theta_2 + \cos^2\phi_1\sin^2\theta_1(\cos^2\phi_2\sin^2\theta_2 - 2\cos^2\theta_2) - \cos\phi_1\cos\phi_2\sin(2\theta_1)\sin(2\theta_2)]\frac{\partial \rho_S(r_1)}{\partial r_1}\frac{\partial \rho_S(r_2)}{\partial r_2} + \rho_S(r_2)(\sin^4\theta_1\cos^4\phi_1 + \cos^4\theta_1 - 6\sin^2\theta_1\cos^2\phi_1\cos^2\theta_1)\left(r_1\frac{\partial^2\rho_S(r_1)}{\partial r_1^2} + \frac{\partial \rho_S(r_1)}{\partial r_1}\right)\right\} \times v(\vec{R} - \vec{r}_1 + \vec{r}_2)\, d\vec{r}_1\, d\vec{r}_2. \tag{B21}$$

The integrals (B17) to (B21) are then calculated only once and the effective potential is then obtained through Eqs. (B3) and (9) in an iterative procedure that converges quickly.

Figure 10 shows the spherical potential and the contributions I_{20} to I_{44} for the deformed one, for the Coulomb and nuclear interactions. In the calculation of the nuclear part, the standard SPP was assumed, but without considering the velocity dependence that arises from Pauli nonlocality, i.e., assuming $v(\vec{R}) = V_0\delta(\vec{R})$ instead of Eq. (6).

APPENDIX C: METHOD TO OBTAIN THE γ ANGLE

In this section, we present the method proposed to obtain the γ angle between $\vec{R}$ and the velocity $\vec{v}$. The method is based on a semiclassical approach to the problem. The velocities of the nuclei (see Fig. 8) can be decomposed into radial and tangential components. Classically, the tangential component, $v\,\sin\gamma$, is related to the angular momentum by

$$L = mvR\sin\gamma \rightarrow \sin^2\gamma = \frac{L^2}{(mvR)^2}. \tag{C1}$$

The velocity of the particles in C1 is half of the relative velocity: $v = v_{\rm REL}/2$. The mass of the particles is related to

the reduced rest mass through

$$m = \frac{m_0}{\sqrt{1 - v^2/c^2}} = \frac{2\mu_0}{\sqrt{1 - v_{\rm REL}^2/4c^2}}. \quad \text{(C2)}$$

Thus, Eq. (C1) can be written as

$$\sin^2\gamma = \left(1 - v_{\rm REL}^2/4c^2\right) \frac{L^2}{(\mu_0 v_{\rm REL} R)^2}. \quad \text{(C3)}$$

Now we assume that $L^2 = \ell(\ell+1)\hbar^2$, and we obtain

$$\sin^2\gamma = \frac{\ell(\ell+1)\hbar^2}{2\mu_0 R^2}\left[\frac{2\left(1 - v_{\rm REL}^2/4c^2\right)}{\mu_0 c^2 v_{\rm REL}^2/c^2}\right]. \quad \text{(C4)}$$

Since the relative velocity is obtained from Eq. (9), we rewrite the above expression as

$$\sin^2\gamma = \frac{\ell(\ell+1)\hbar^2}{2\mu_0 R^2}\left\{\frac{1}{K(R)[1 + K(R)/8\mu_0 c^2]}\right\}, \quad \text{(C5)}$$

where the local kinetic energy is given by

$$K(R) = E_{\rm CM} - V_D(R). \quad \text{(C6)}$$

At low bombarding energies, for which $K(R) \ll 8\mu_0 c^2$, Eq. (C5) is rewritten as

$$\sin^2\gamma = \frac{\ell(\ell+1)\hbar^2}{2\mu_0 R^2}\frac{1}{K(R)}. \quad \text{(C7)}$$

We have assumed (C7) to calculate the contributions of Eqs. (B15) and (B16) to the deformed potential. Clearly, Eq. (C7) implies that the effective potential is ℓ dependent.

We point out that Eq. (C7) can lead to $\sin^2\gamma < 0$ or $\sin^2\gamma > 1$. The case $\sin^2\gamma < 0$ occurs when $K(R) < 0$, which involves a classically forbidden region of R values (tunneling of the s-wave barrier). In this case, we are dealing with sub-Coulomb energies and thus with very small velocities. Therefore, the effects of relativity are negligible in this region and the value assumed for $\sin^2\gamma$ is, in fact, not important in this case. The other case, $\sin^2\gamma > 1$, occurs when

$$\frac{\ell(\ell+1)\hbar^2}{2\mu_0 R^2} > K(R). \quad \text{(C8)}$$

Obviously, values corresponding to $\sin^2\gamma > 1$ sound strange and one could worry about the respective effect on the calculations. However, Eq. (C8) is equivalent to

$$V_D(R) + \frac{\ell(\ell+1)\hbar^2}{2\mu_0 R^2} > E_{\rm CM}, \quad \text{(C9)}$$

which is also a region of R values forbidden classically (tunneling of the ℓ-wave barrier). Of course, regions (of R and ℓ) for which $\sin^2\gamma \gg 1$ are thus not probed by the elastic scattering process. Furthermore, in this region the nuclear and Coulomb potentials are negligible in comparison with the (large) centrifugal one. Therefore, the value assumed for $\sin^2\gamma$ is also not important in this case.

[1] L. C. Chamon, B. V. Carlson, L. R. Gasques, D. Pereira, C. De Conti, M. A. G. Alvarez, M. S. Hussein, M. A. Candido Ribeiro, E. S. Rossi Jr., and C. P. Silva, Phys. Rev. C **66**, 014610 (2002).

[2] L. C. Chamon, B. V. Carlson, and L. R. Gasques, Phys. Rev. C **83**, 034617 (2011).

[3] V. M. Datar, S. Kumar, D. R. Chakrabarty, V. Nanal, E. T. Mirgule, A. Mitra, and H. H. Oza, Phys. Rev. Lett. **94**, 122502 (2005).

[4] K. Langanke and C. Rolfs, Z. Phys. A **324**, 307 (1986).

[5] K. Langanke and C. Rolfs, Phys. Rev. C **33**, 790 (1986).

[6] P. Mohr*et al*, Z. Phys. A **349**, 339 (1994).

[7] S. A. Afzal, A. A. Z. Ahmad, and S. Ali, Rev. Mod. Phys. **41**, 247 (1969).

[8] H. Friedrich, Phys. Rep. **74**, 209 (1981).

[9] B. Buck, H. Friedrich, and C. Wheatley, Nucl. Phys. A **275**, 246 (1977).

[10] L. C. Chamon, D. Pereira, M. S. Hussein, M. A. Candido Ribeiro, and D. Galetti, Phys. Rev. Lett. **79**, 5218 (1997).

[11] M. A. Candido Ribeiro, L. C. Chamon, D. Pereira, M. S. Hussein, and D. Galetti, Phys. Rev. Lett. **78**, 3270 (1997).

[12] H. De Vries, C. W. De Jager, and C. De Vries, At. Data Nucl. Data Tables **36**, 495 (1987).

[13] J. L. Russel Jr., G. C. Phillips, and C. W. Reich, Phys. Rev. **104**, 135 (1956).

[14] G. A. Lalazissis, J. König, and P. Ring, Phys. Rev. C **55**, 540 (1997).

[15] T. Niksic, D. Vretenar, P. Finelli, and P. Ring, Phys. Rev. C **66**, 024306 (2002); D. Vretenar, T. Niksic, and P. Ring, *ibid.* **68**, 024310 (2003).

[16] N. P. Heydenburg and G. M. Temmer, Phys. Rev. **104**, 123 (1956).

[17] R. Nilson, W. K. Jentschke, G. R. Brigs, R. O. Kerman, and J. N. Snyder, Phys. Rev. **109**, 850 (1958).

[18] T. A. Tombrello and L. S. Senhouse, Phys. Rev. **129**, 2252 (1963).

[19] W. S. Chien and Ronald E. Brown, Phys. Rev. C **10**, 1767 (1974).